Phase Relations, Quasicontinuous Spectra and Subfemtosecond Pulses in High-Order Stimulated Raman Scattering with Short-Pulse Excitation

V. P. Kalosha* and J. Herrmann

Max Born Institute for Nonlinear Optics and Short Pulse Spectroscopy, Max-Born-Strasse 2a, D-12489 Berlin, Germany

(Received 14 February 2000)

High-order stimulated Raman scattering for pumping by ps and sub-ps pulses is studied in the frame of a time-domain approach without the slowly varying envelope approximation. Formation of pulse trains with sub-fs durations in the ps-pump regime is demonstrated using external phase compensation. For sub-ps excitation a novel broadening mechanism of Raman lines is predicted that leads to a quasicontinuous spectrum and permits one to generate single sub-fs pulses. We predict also essential shortening of a delayed fs-probe pulse by the Raman oscillations without phase control.

PACS numbers: 42.65.Re, 42.65.Dr, 42.65.Tg

Recent advances in ultrafast laser technology have made possible the generation of pulses shorter than 5 fs [1]. Different concepts such as utilization of high-order harmonic generation [2], ultrawide spectral broadening by self-phase modulation [3], and pulse splitting in resonant medium [4] are under development to overcome this barrier and to reach the sub-fs region. Another interesting possibility is the use of high-order stimulated Raman scattering (HSRS). This process provides a tremendously broad spectrum with many lines spreading from the far IR to the extreme UV [5]. The potential of HSRS for sub-fs pulse generation has been studied previously in the framework of different models. Yoshikawa *et al.* first proposed to apply HSRS for short-pulse generation using the assumption that all Raman lines are phase locked [6]. Kaplan considered the possibility of multicomponent Raman solitons [7]. Harris and Sokolov suggested the use of electromagnetically induced transparency to produce trains of sub-fs pulses by cw two-color laser beams [8]. In the present Letter a study of HSRS for pumping with ps and sub-ps pulses is presented based on the time-domain approach without the use of the slowly varying envelope approximation (SVEA). The previously applied frequency-domain approach based on SVEA [6–9] is inadequate for short-pulse pumping where the spectral phases of the Raman lines change too rapidly or their bandwidths are not small compared with the Raman frequency. Note that short-pulse pumping is best suited for effective high-intense excitation relevant to recent experiments [5,10]. First, we present a new analytical solution for HSRS which describes formation of pulse trains or single-pulse shortening and broad-band spectra. Then we numerically solve the basic equations accounting for linear dispersion in the broad spectral range (without Taylor expansion), Stark shift, and Kerr effect to find limitations and optimum conditions under real physical conditions. We show that for ps-pulse pumping trains with chirped pulses not shorter than ≈ 2 fs are generated. If the phase is subsequently compensated by a liquid-crystal spatial light modulator (LQSLM), these pulses can be shortened below 1 fs. For sub-ps input pulses, we show a novel mechanism for the generation of quasicontinuous spectra in HSRS, which yields the possibility to generate single sub-fs pulses. We explore also a single-pulse shortening of a fs-probe pulse without external phase control by Raman oscillations excited by two-color ps-pump pulses.

We consider the propagation of incident pump pulse through a Raman-active medium. The medium response is described by polarization P separated into the contributions from the Raman process P_R, the linear dispersion P_L, and the electronic Kerr effect P_K. The dynamics of the Raman polarization $P_R = N\mathrm{Sp}(\hat{\alpha}\hat{\rho})E$ is determined by the two-photon density-matrix equation [11]:

$$\left(\frac{\partial}{\partial t} + \frac{1}{T_2} - i\Omega\right)\rho = \frac{i}{2\hbar}[(\alpha_{11} - \alpha_{22})\rho + \alpha_{12}w]E^2, \tag{1}$$

$$\frac{\partial w}{\partial t} + \frac{w+1}{T_1} = \frac{i}{2\hbar}\alpha_{12}(\rho - \rho^*)E^2, \tag{2}$$

where $\rho \equiv \rho_{12} = \frac{1}{2}(u + iv)$ is the nondiagonal element of the density matrix, $w = \rho_{22} - \rho_{11}$ is the population difference, $E(z,t)$ is the field strength, Ω is the Raman frequency shift, and $\hat{\alpha}$ is the two-photon polarizability matrix with nondiagonal and diagonal elements responsible for the Raman process and Stark shift, respectively. T_1 and T_2 are the polarization and population relaxation times, respectively. The Fourier component of the linear polarization is given by $P_L(\omega, z) = \epsilon_0\chi(\omega)E(\omega, z)$, where the susceptibility $\chi(\omega)$ will be described by the Sellmeyer formula $\chi(\omega) = \sum_\ell S_\ell(\omega_\ell^2 - \omega^2)^{-1}$ with experimentally determined parameters S_ℓ, ω_ℓ. For intense short pulses Kerr effect with polarization $P_K = \epsilon_0\chi^{(3)}E^3(t)$ plays a role as competition to SRS.

With this model for the polarization the propagation of a linearly polarized wave in the nonlinear medium is described by the wave equation. The electric field is assumed to be uniform along the transverse axis, as it is realized in hollow waveguides filled with the Raman medium [10]. It can be proved by the method of characteristics that the

 0031-9007/00/85(6)/1226(4)$15.00

wave equation is reduced to the following equation describing waves traveling in the forward direction only [12]:

$$\frac{\partial E}{\partial z} = -\frac{c\mu_0}{2}\frac{\partial P}{\partial \eta}, \tag{3}$$

where $\eta = t - z/c$ is the moving time. The condition for the neglect of backscattering is given by $\xi_{\mathcal{M}} = \max|P_{\mathcal{M}}/\epsilon_0 E| \ll 1$ ($\mathcal{M} = R, L, K$). For parameters given below the corrections to Eq. (3) are $\xi_R, \xi_L \sim 10^{-3}$, and $\xi_K \sim 10^{-5}$, i.e., it holds true with high accuracy.

In order to obtain better insight, we first search for an analytical solution of Eqs. (1) and (3), neglecting dispersion, Stark shift, Kerr effect, relaxation and population changing ($w = -1$), and consider the case of a two-color excitation by two input pulses with a frequency difference Ω. Then the solution of Eq. (1) is given by $\rho = \rho_0 \exp(i\Omega\eta)$, where $\rho_0 = -i\alpha_{12}\int_{-\infty}^{\eta} E^2(z,\eta') \times \exp(-i\Omega\eta')\,d\eta'/2\hbar$ depends weakly on time and distance. For a simplified analysis we assume $\rho_0 \approx$ const. The quasi-steady-state behavior of ρ_0 will be supported by the numerical results [see, e.g., Fig. 2(a) below]. Substituting $P = N\alpha_{12}u_0 \sin(\Omega\eta)E$ with $u_0 =$ const into Eq. (3), the solution can be found as follows:

$$E(z,\eta) = E_0(s)\sin(\Omega s)/\sin(\Omega\eta), \tag{4}$$

where $s = s(z,\eta)$ is determined from the relation $\mathrm{tg}(\Omega s/2) = \mathrm{tg}(\Omega\eta/2)\exp(-\gamma z)$. Here $E_0(\eta)$ is the input field at $z = 0$ and $\gamma = \frac{1}{2}c\mu_0 N\alpha_{12}\Omega u_0$. For the limiting case $\gamma z \ll 1$ we obtain $s \approx \eta - \gamma z \sin(\Omega\eta)/\Omega$ and Eq. (4) gives frequency-modulated, but not shortened pulses with a small number of Raman lines in spectrum which has a Bessel-like distribution. The field strength of the lines shows periodic sign changes on the anti-Stokes side, i.e., their phases jump between 0 and π and they are not phase locked. For the regime of adiabatic eigenstates the analogous solution was obtained in Ref. [8]. However, for sub-fs pulses a large number of Raman lines (i.e., $\gamma z > 1$) is required. In this more interesting case assuming $\Gamma = \exp(\gamma z) \gg 1$ the field is zero everywhere except in the vicinity of $\eta = \eta_n = \pi(2n+1)/\Omega$ ($n = 0, \pm 1, \ldots$), where $s = \Gamma\eta + (1-\Gamma)\eta_n$. Then Eq. (4) describes a pulse train with repetition period $2\pi/\Omega$, pulse duration $2\pi/\Omega\Gamma$, and maximal frequency and maximal field strength growing with Γ. In Fig. 1 the solution (4) is represented for two 200-fs Gaussian pulses as the input field which agrees well with these estimations even for $\gamma z = 1.2$. The train of shortened frequency-modulated pulses shows a double-peak structure which arises from superposition of the two-color input waves. The spectrum in Fig. 1(b) has a large number of Raman lines which are not phase locked at either the Stokes or the anti-Stokes side. However, in the region of large γz, additional effects not taken into account in the solution (4) play a significant role and require more complex numerical simulations.

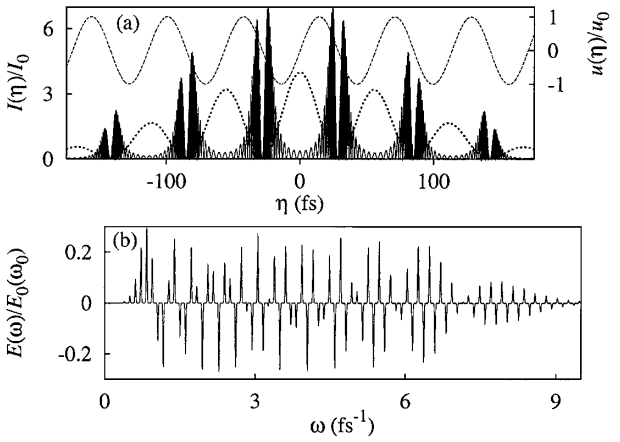

FIG. 1. Temporal and spectral characteristics of the solution (4) for $\gamma z = 1.2$ and two-color excitation by two 200-fs pulses with frequencies $\omega_0 = 2\pi c/\lambda_0$ and $\omega_0 - \Omega$, where $\lambda_0 = 790$ nm and $\Omega = 587$ cm^{-1}: (a) pulse shape (solid curve), polarization (dashed curve), and envelope of the input pulses (dotted curve); (b) spectrum (solid line).

The basic equations (1)–(3) were solved numerically for the following parameters of rotational Raman transition in molecular H_2 [5,6,9]: $\Omega = 587$ cm^{-1}, $N = 5.4 \times 10^{20}$ cm^{-3} (20 atm), $(\alpha_{12}, \alpha_{11}, \alpha_{22}) = (1.3, 9.95, 10.44) \times 10^{-41}$ C m^2/V, $\chi^{(3)} = 1.65 \times 10^{-24}$ (m/V)^2, $(S_1, S_2) = (1.45, 1.19)$ fs^{-2}, $(\omega_1, \omega_2) = (20.0, 25.7)$ fs^{-1}, $T_1 = 1$ ns, and $T_2 = 100$ ps. We used a split-step Fourier method and performed nonlinear steps by the fourth-order Runge-Kutta method for field updating in space and for integration of Eqs. (1) and (2). First we consider the results for the case of transient two-color excitation by 1-ps pulses which allows efficient excitation for pump intensities, for which the influence of Kerr effect is still not dominant. Figure 2 shows a train of frequency-modulated pulses with pulse duration of about 2 fs together with the molecular polarization $u(\eta)$ for the full model Eqs. (1)–(3) with dispersion and Kerr effect. The spectrum in Fig. 2(b) shows slightly broadened discrete Raman lines extended from IR up to the UV, which are not phase locked. Note that longer distances or higher input intensities lead to an irregular pulse train with additional intermediate pulses which are not shorter than in Fig. 2(a). Sub-fs pulses can be achieved when the spectral phases are compensated for by the application of a broad-band modulator. The result of ideal phase compensation with reduced numbers of shortened pulses is shown in Fig. 2(c). In spite of the transient condition $\tau < T_2$ the molecular dynamics for $u(\eta)$ and $w(\eta) \approx -1$ in Fig. 2(a) shows a quasi-steady-state behavior caused by the onset of large frequency modulations in the field. Note that here the density matrix cannot be described by adiabatically eigenstates as considered in Ref. [8].

For applications the generation of single sub-fs pulses is of greater interest than that of pulse trains with the very high repetition rate. But the discrete line structure in HSRS necessarily leads to pulse trains. However we

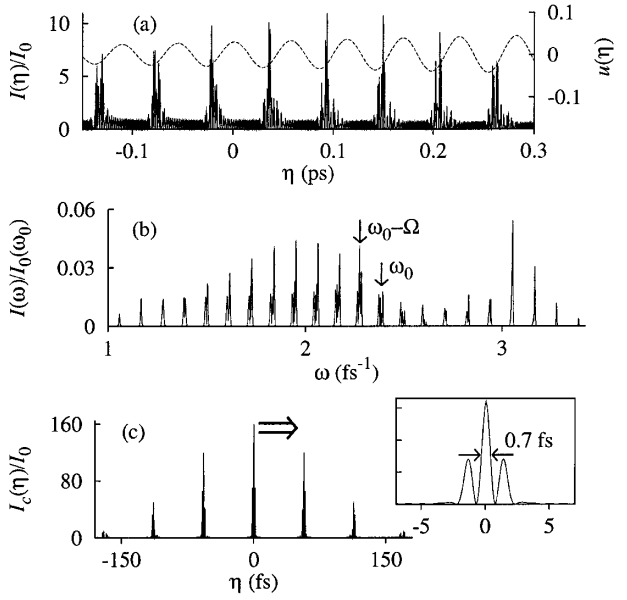

FIG. 2. Pulse train and spectrum for ps-pulse excitation: (a) pulse shape (solid curve) and polarization (dashed curve), (b) spectrum, (c) pulse train after perfect phase compensation for two 1-ps input pulses with intensity $I_0 = 2 \times 10^{11}$ W/cm^2 and frequencies as in Fig. 1 [shown by arrows in (b)] at $z = 10$ cm. Inset shows the central compressed pulse.

found an excitation regime with sub-ps input pulses which shows a novel type of line broadening with quasicontinuous spectra. As an example in Fig. 3 the results are presented for the case of a two-color excitation of rotational Raman lines in H_2 by 200-fs pulses. For the case of pure HSRS at two different distances, the central part of the output pulse train in Fig. 3(a) shows well-separated frequency-modulated pulses, the shortest pulse duration is about 2 fs. Owing to the influence of dispersion and Kerr effect, the pulses become more irregular and longer as shown in Fig. 3(b). In the evolution of spectra for short distances, we found separated Raman lines. But with increasing propagation length, the linewidth increases and the spectrum finally becomes quasicontinuous. This can be seen in Fig. 4(a) for pure HSRS and in Fig. 4(b) with the account of dispersion and Kerr effect. The physical origin of this effect is not related to previously investigated much weaker line-broadening mechanisms in SRS or with the Kerr effect. The extremely large broadening here is caused by the reaction of the highly frequency-modulated pulses inside the train on the molecular oscillations leading to a frequency modulation of the Raman response of the kind $u = u_0 \sin[\Omega\eta + \psi(\eta)]$. This can be seen in the lower part of Fig. 3(a), where besides the numerically calculated Raman response $u(\eta)$ (dotted line), oscillations without phase modulation $u = u_0 \sin(\Omega\eta)$ are shown by the pointed line, which demonstrates the chirp $\psi(\eta)$. Continuous spectrum in H_2 excited by sub-ps pulses has been already observed, but it was interpreted by the action of the Kerr effect [5].

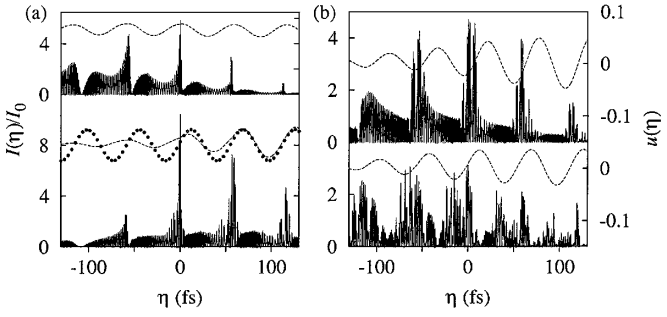

FIG. 3. Pulse trains for sub-ps excitation at distance 10 (higher) and 25 cm (lower) without (a) and with (b) account of dispersion and Kerr effect in H_2 for two-color excitation by 200-fs pulses with intensity $I_0 = 10^{12}$ W/cm^2 and frequencies as in Fig. 1.

The behavior of the spectral phases $\varphi(\omega)$ of the field is of crucial importance for pulse shortening. For pure HSRS $\varphi(\omega)$ shows a negative group-velocity dispersion (GVD) in the main part of the spectrum [dotted curve in Fig. 4(a)]. Figure 4(b) shows the additional influence of normal dispersion and Kerr effect of H_2; now the change of the spectral phase on the Stokes side becomes smaller with a smaller negative GVD while on the anti-Stokes side the positive GVD increases. In order to generate single sub-fs pulses, an external broad-band modulator with phase function $\varphi_c(\omega)$ can be applied after the pulse has passed the Raman medium. In Fig. 4(c) the dotted line shows the pulse $I_c(\eta)$ after action of an ideal compressor with perfect phase compensation. As a possible candidate for a real broad-band pulse compressor we consider a LQSLM [13] with 256 independently controlled pixels and a transmission range between 0.4 and 1.8 μm. As seen in the

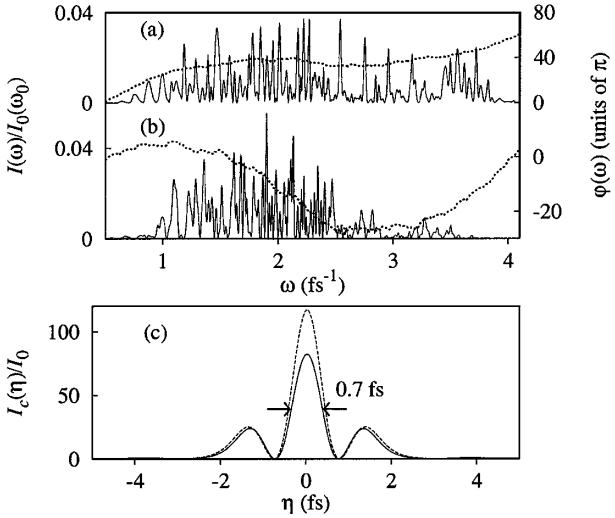

FIG. 4. Spectrum (solid curve) and spectral phase (dotted curve) for sub-ps excitation without (a) and with (b) account of dispersion and Kerr effect; (c) single sub-fs pulse after phase compensation of the spectrum shown in (b) by a modulator with 256 pixels (solid curve) and an ideal compressor (dashed curve). Distance is 25 cm and other parameters are as in Fig. 3.

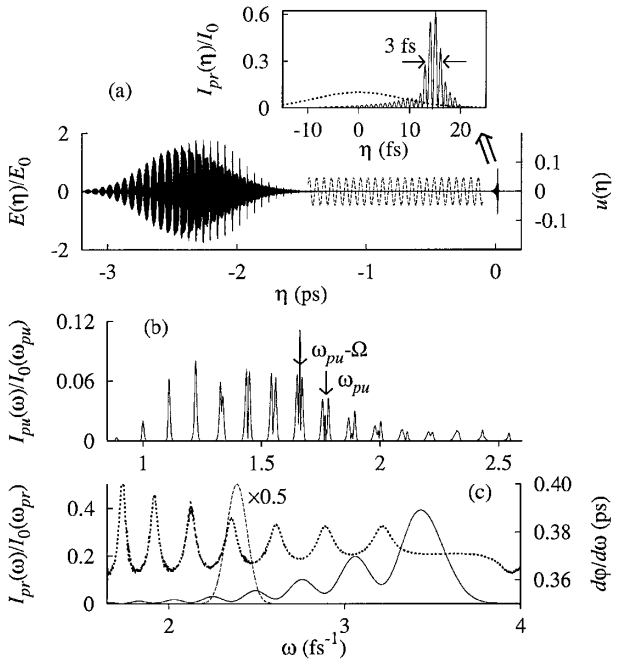

FIG. 5. Pulse shortening of a delayed probe pulse at distance 5 cm. (a) Field strength (solid curve) and polarization (dashed curve) for pumping by two 0.5-ps, 5×10^{11}-W/cm^2 pulses with wavelengths $\lambda_{\mathrm{pu}} = 1064$ and 1135 nm and 20-fs, 5×10^{10}-W/cm^2 probe pulse with wavelength $\lambda_{\mathrm{pr}} = 790$ nm; (b) pump pulse spectrum; (c) probe pulse spectrum (solid curve) and phase delay (dotted curve) along with its initial spectrum (dashed curve). Inset shows the shortened 3-fs probe pulse shape (solid curve) and its initial envelope (dotted curve).

solid line in Fig. 4(c), by using such active control of the spectral phases, a single almost half-cycle pulse with a duration of 0.7 fs and a side maxima below 20% of the main maximum can be generated.

Finally we found a regime which can be used as a novel pulse shortening method by HSRS with compression below 5 fs without any external phase control. In this method two-color ps-pump pulses excite a Raman-active medium. A delayed weaker fs-probe pulse, with duration $\tau_{\mathrm{pr}} = 20$ fs, interacts with the long-living Raman excitation and experiences a large spectral broadening and shortening. In Fig. 5(a) the pulse train formed within the pump pulses, the Raman oscillations $u(\eta)$, and the shortened 3-fs probe pulse are shown after propagation through H_2 with account of dispersion and Kerr effect. The spectrum of the pump pulses [Fig. 5(b)] consists of discrete Raman lines similar to those in Fig. 2(b). But the spectrum of the probe pulse plotted in Fig. 5(c) shows a continuous broadening and a large shift to the anti-Stokes side. The dotted line shows a constant delay within all spectral maxima, i.e., the output probe pulse is nearly phase locked automatically without external phase control. A larger propagation distance or higher input intensities do not lead to shorter pulses because of the decrease of the molecular oscillations and the counteraction of the Kerr effect. The solution (4) gives also an understanding of the probe pulse compression by the excited Raman medium. Now u_0 is mainly determined by the pump and for $\tau_{\mathrm{pr}} < 2\pi/\Omega$ and $\Gamma \gg 1$ we find as above $s = \Gamma\eta + s_0$, where s_0 depends on the delay between pump and probe. For optimum delay $\eta_D = \pi(2n + 1)/\Omega$ Eq. (4) yields the asymptotic solution for a single pulse of the form $E_{\mathrm{pr}}(z, \eta) = \Gamma E_{\mathrm{pr}}[z = 0, \Gamma(\eta - \eta_D)]$. Now the output pulse duration is related not to Ω as for longer pulses but is given by $\tau_{\mathrm{pr}}/\Gamma$ and the maximal frequency by $\Gamma\omega_{\mathrm{pr}}$. With the parameters in Fig. 5 we have $\gamma z = 1.75$ and a pulse-shortening factor $\Gamma = 5.75$ which is well in agreement with the numerical solution. The pulse compression method by HSRS in hollow waveguides studied here is experimentally much simpler than pulse shortening by self-phase modulation because of the superfluous phase control. Further, the continuous shift of spectrum to higher frequencies is of interest for wavelength conversions.

We gratefully acknowledge support from the DFG, Project No. He2083/5-1, partial support by BMBF, Project No. WEI-001-98, and INTAS, Project No. 97-2018.

*Email address: kalosha@mbi-berlin.de

[1] A. Baltuška *et al.,* Opt. Lett. **22**, 102 (1997); M. Nisoli *et al.,* Opt. Lett. **22**, 522 (1997).
[2] P. Antoine, A. L'Huillier, and M. Lewenstein, Phys. Rev. Lett. **77**, 1234 (1996); K. J. Schafer and K. C. Kulander, Phys. Rev. Lett. **78**, 638 (1997).
[3] V. P. Kalosha and J. Herrmann, Phys. Rev. A **62**, 011804 (2000).
[4] V. P. Kalosha and J. Herrmann, Phys. Rev. Lett. **83**, 544 (1999).
[5] H. Kawano, Y. Hirakawa, and T. Imasaka, IEEE J. Quantum Electron. **34**, 260 (1998); V. Krylov *et al.,* J. Opt. Soc. Am. B **15**, 2910 (1998).
[6] S. Yoshikawa and T. Imasaka, Opt. Commun. **96**, 94 (1993); H. Kawano *et al.,* Phys. Rev. A **59**, 4703 (1999).
[7] A. E. Kaplan, Phys. Rev. Lett. **73**, 1243 (1994).
[8] S. E. Harris and A. V. Sokolov, Phys. Rev. Lett. **81**, 2894 (1998).
[9] F. L. Kien *et al.,* Phys. Rev. A **60**, 1562 (1999).
[10] A. Nazarkin *et al.,* Phys. Rev. Lett. **83**, 2560 (1999).
[11] V. S. Butylkin, A. E. Kaplan, Y. G. Khronopulo, and E. I. Yakubovich, *Resonant Nonlinear Interactions of Light with Matter* (Springer-Verlag, New York, 1977).
[12] R. K. Bullough *et al.,* Phys. Scr. **20**, 364 (1979).
[13] A. M. Weiner, Prog. Quantum Electron. **19**, 161 (1995).